Antiviral Research 166 (2019) 1–10

Contents lists available at ScienceDirect

Antiviral Research

journal homepage: www.elsevier.com/locate/antiviral

Aberrant PD-1 ligand expression contributes to the myocardial inflammatory injury caused by Coxsackievirus B infection

Tianying Wang[a,c,1], Shuang Chen[b,c,1], Xueqing Wang[a,c,e], Yike Huang[d], Jianfa Qiu[a,c], Yanru Fei[a,c], Anita Chaulagain[a,c], Yang Chen[a,c], Yan Wang[a,c], Lexun Lin[a,c], Biying Yan[a,c], Ying Wang[a,c], Wei Wang[e], Wenran Zhao[d,**], Zhaohua Zhong[a,c,*]

[a] Department of Microbiology, Harbin Medical University, Harbin, China
[b] Department of Immunology, Harbin Medical University, Harbin, China
[c] Heilongjiang Key Laboratory of Immunity and Infection, Harbin, China
[d] Department of Cell Biology, Harbin Medical University, Harbin, China
[e] School of Medical and Health Sciences, Edith Cowan University, Perth, Australia

ARTICLE INFO

Keywords:
Coxsackievirus B3
Programmed cell death ligand 1
Programmed cell death ligand 2
AU-rich element binding protein 1
Immunotherapy

ABSTRACT

Coxsackievirus group B (CVB) is considered as one of the most common pathogens of human viral myocarditis. CVB-induced myocarditis is mainly characterized by the persistence of the virus infection and immune-mediated inflammatory injury. Costimulatory signals are crucial for the activation of adaptive immunity. Our data reveal that the CVB type 3 (CVB3) infection altered the expression profile of costimulatory molecules in host cells. CVB3 infection caused the decrease of PD-1 ligand expression, partially due to the cleavage of AU-rich element binding protein AUF1 by the viral protease $3C^{pro}$, leading to the exacerbated inflammatory injury of the myocardium. Moreover, systemic PD-L1 treatment, which augmented the apoptosis of proliferating lymphocytes, alleviated myocardial inflammatory injury. Our findings suggest that PD1-pathway can be a potential immunologic therapeutic target for CVB-induced myocarditis.

1. Introduction

Coxsackievirus group B (CVB) is a nonenveloped positive single-stranded RNA virus belonging to the *Enterovirus* genus of *Picornaviridae* (Cheung et al., 2002; Garmaroudi et al., 2015; Jubelt and Lipton, 2014; Marchant et al., 2008). It is one of the most common pathogens that cause human viral myocarditis (VCM) (Rose, 2016). CVB infection is a principle etiologic agent of human acute myocarditis (Heymans et al., 2016). Pancreatitis and aseptic meningitis are also frequently associated with the infection of enteroviruses, including CVB (Jubelt and Lipton, 2014). CVB-induced myocarditis is characterized by the persistence of the inflammation with leukocyte infiltration in the myocardium (Fairweather and Rose, 2007; Rose, 2016), which may lead to dilated cardiomyopathy (Fairweather et al., 2012). CVB-induced myocarditis is usually life-threatening in newborns (Duncan et al., 2001; Knowlton et al., 1996; Woodruff, 1980) with considerable neonatal morbidity and mortality (Durani et al., 2010).

Myocarditis induced by CVB is proposed to be the consequence of the direct damage to the myocardium by viral replication combined with the adverse effect of the host-antiviral immunity (Liao et al., 2015). Immune-mediated inflammation is thought to be one of the primary mechanisms for the myocardial damage induced by viral infection (Kim et al., 2001; Marchant et al., 2008). However, the immune response against CVB is still poorly understood. T cells play a central role in cell-mediated immunity (Frisancho-Kiss et al., 2007; Kim et al., 2007). Both antigen recognition signal which is provided by the interaction of the antigenic peptide-major histocompatibility complex (MHC) with the T cell receptor (TCR), and costimulatory signal which is generated by the binding of B7 ligands to the CD28 family on lymphocytes, are crucial for the activation of naïve T cells (Fairweather et al., 2005; Huang and Yang, 2009; Rose, 2011; Yajima and Knowlton, 2009). The programmed cell death protein 1 (PD-1), a receptor in the CD28 family, has been well characterized as a negative regulator of T cells that delivers inhibitory signal to T cells (Paiva et al., 2015; Ray et al., 2015; Sponaas et al., 2015; Tamura et al., 2013). Interactions between PD-1 and programmed cell death ligands, also known as PD-L1

* Corresponding author. Department of Microbiology, Harbin Medical University, Harbin, China.
** Corresponding author.
E-mail addresses: zhaowr@hrbmu.edu.cn (W. Zhao), zhongzh@hrbmu.edu.cn (Z. Zhong).
[1] These authors contribute equally to the work.

https://doi.org/10.1016/j.antiviral.2019.03.007
Received 31 October 2018; Received in revised form 14 March 2019; Accepted 16 March 2019
Available online 20 March 2019
0166-3542/

(B7H1; CD274) and PD-L2 (B7-DC; CD273), which are expressed on various tissues and on antigen-presenting cells (APCs) that present self-antigens, can activate the cytoplasmic immunoreceptor tyrosine-based inhibitory motif (ITIM) of PD-1, and which inhibits the activation and proliferation of T cells (Hong et al., 2018). Thus, PD-L1 and PD-L2 are potent molecules that can prevent the generation of self-reactive T effector cells and promote the differentiation of $CD4^+CD25^+Foxp3^+$ Treg cells (Frisancho-Kiss et al., 2007; Kmieciak et al., 2009). It has also been shown that PD-L1 and PD-L2 suppress the expansion of escaping of the self-reactive T cells and prevent autoimmunity (Hong et al., 2018). PD-1-deficient C57BL/6 mice develop severe lupus-like glomerulonephritis and progressive arthritis (Guo et al., 2014), indicating that PD-1 functions as a key molecule in the development of autoimmune diseases (Sharpe and Pauken, 2018). Meanwhile, PD-L1 is highly expressed on a variety of tumors and usually is associated with poor clinical prognosis. Therapeutic blockade of this pathway using anti-PD-1/PD-L1 monoclonal antibodies, is effective in promoting antitumor immunity, and has taken the central stage in immunotherapies for cancer after multiple clinical successes (Lesokhin et al., 2016; Lipson et al., 2013).

Previously, we reported that the protease 3C ($3C^{pro}$) of CVB contributed to the cleavage of AUF1, an RNA-binding protein of the host cells. Cleaving AUF1 may be a strategy employed by CVB to enhance the stability of its genome and to influence the immune microenvironment (Wong et al., 2013). We found that CVB infection led to a dramatic downregulation of the negative costimulatory molecules, which were also partially associated with the $3C^{pro}$-induced cleavage of AUF1. In this study, we have evaluated the effect of CVB infection on the expression of costimulatory molecules PD-L1 and PD-L2 in infected cells and the interaction between CVB and PD-1 ligands. Our results provide novel insight into the immune mechanism involved in the myocardial injury caused by CVB. This study may also shed light for the prevention and treatment of viral myocarditis through manipulating immunologic targets.

2. Materials and methods

2.1. Cell culture, virus and mouse

Cells were cultured in high-glucose Dulbecco's modified Eagle's medium (DMEM) (Gibco, Invitrogen, Cat# 11965-084, USA) containing 10% inactivated fetal bovine serum (FBS, Biotechnology, Israel) and penicillin-streptomycin (100 IU/ml-μg/ml) (Gibco, Invitrogen, Cat# 15070063, USA). Cells were maintained at 37 °C and 5% CO_2. When cell confluency reached 80%–90%, the cells were washed with PBS twice and treated with 0.25% Trypsin-EDTA (Gibco, Invitrogen, Cat# 25200056, USA). The second-passage of the cells were reseeded in culture dishes at an appropriate density.

Balb/c mice were purchased from the Experimental Animal Center of Harbin Medical University, Harbin, China. All procedures involving in animals were approved by the Ethics Committee of Harbin Medical University in accordance with the Regulation for the Use of Laboratory Animals at Harbin Medical University.

EGFP-CVB3, which expresses enhanced green fluorescence protein (EGFP), was constructed previously by our laboratory based on pMKS1, a plasmid containing the full-length CVB3 genomic complementary DNA (cDNA) (Tong et al., 2011). The virus virulence was examined by $TCID_{50}$ as described previously (Malenovska, 2013).

2.2. Plasmid construction

EGFP-labeled AUF1 isoforms (Accession: NM_031370, NM_031369, NM_002138, and NM_001003810) expression vectors were constructed previously (Wong et al., 2013). The pcDNA3.1$^+$-EGFP vector was modified by inserting a linker sequence between the EGFP sequence and the multiple cloning site (MCS) to ensure noninterference between EGFP and the inserted portion. As the four AUF1 isoforms share the same first and last exons, we designed one pair of primers to amplify the four isoform sequences by PCR assay. The primer sequences are listed in Supplementary Table 2. All four isoforms were separated through DNA agarose gel electrophoresis, and the *Hind* III and *Kpn*I restriction enzyme sites were used for terminal digestion. Then, the four isoform fragments were purified from the gel and inserted into the pcDNA3.1$^+$-EGFP vectors, which were designated as EGFP-AUF1 p45, EGFP-AUF1 p42, EGFP-AUF1 p40, and EGFP-AUF1 p37, respectively.

2.3. Plasmids and siRNA transfection

Plasmids were extracted with an Axygen AxyPrep Plasmid Midiprep Kit (Cat# AP-MD-P-10, Corning, NY). Two AUF1-specific siRNAs targeting exon 3 and 5 were designed and synthesized by GenePharma (Shanghai, China) (Supplementary Table 2). To avoid potential off-target effects, two siRNAs were mixed and simultaneously transfected into cells. Lipofectamine 2000 (Invitrogen, Carlsbad, CA) was used to transfect the plasmids and siRNAs according to the manufacturer's instruction.

2.4. Western blotting

Whole cell extracts were lysed by incubation with RIPA buffer (Pierce Biotechnology, Rockford, IL) containing PMSF for 30 min on ice and vortexed 5–6 times during the incubation. After centrifugation at 12,000 rpm for 15 min at 4 °C, the supernatants were collected and quantified by bicinchoninic acid assays (BCA kit; Cat# AR0146, Boster, Wuhan, China). After separation with SDS-PAGE electrophoresis, the proteins were transferred to a 0.22 μm PVDF membrane, followed by blocking in 5% nonfat milk. The targets were blotted with antibodies including polyclonal anti-PD-L1 antibodies (1:200 dilution, Cat# 17952-1-AP, Proteintech, Wuhan, China; 1:500 dilution, Cat# ab238697, Abcam, Cambridge, MA), polyclonal anti-PD-L2 antibody (1:500 dilution, Cat# 18251-1-AP, Proteintech, Wuhan, China), polyclonal anti-AUF1 antibody (1:1000 dilution, Cat# ab61193, Abcam), monoclonal anti-β-actin antibody (1:3000, Cat#TA811000, OriGene, Rockville, MD), or monoclonal anti-VP1 antibody (1:3000, Cat#5-D8/1, DAKO, Denmark). PVDF membranes were incubated with the corresponding primary antibodies overnight at 4 °C. After being washed with Tris-buffered saline containing 1% Tween-20 (TBST; 20 mM Tris-Cl, pH 7.5, 0.5 mol/L NaCl, 0.05% Tween-20) three times, the membranes were then incubated with horseradish peroxidase (HRP)-conjugated secondary antibodies at room temperature for 1 h. A Novex ECL Chemiluminescent Substrate Reagent kit (Cat# WP20005, Invitrogen, U.S) was used to visualize the blots. The grayscale value of the blots was analyzed with ImageJ software.

2.5. mRNA stability

To measure RNA stability, HeLa cells were seeded in 24-well plates and cultured until 70%–80% confluence. AUF1 was overexpressed by transfecting cells with EGFP-AUF1 for 24 h or knocked down with siRNAs for 48 h. The cells were treated with actinomycin D (ActD) (10 μg/ml) for 30 min before harvest. Total RNA was extracted with TRIzol reagent (Cat# 15596018, Invitrogen, U.S) according to the manufacturer's protocol. RNA concentrations were examined with a Nanodrop 2000 (ThermoFisher, U.S). RNA samples were first treated with gEraser and then by reverse transcription PCR (RT-PCR) with a PrimeScript 1st Strand cDNA Synthesis kit (TaKaRa, Cat# RR047A, Dalian, China) for reverse transcription. The total reaction volume for the reverse transcription reaction was 10 μl, in which 1 μl oligo-dT (50 μM), 1 μl RNA template, 2 μl 5 × PrimeScript buffer, 5.5 μl RNase free H_2O, and 0.5 μl PrimeScript RTase (200 U/μl) were added and mixed well. Reverse transcription was carried out for 15 min at 37 °C and followed by 5 s at 85 °C to inactive the enzyme using a DNA Engine Peltier Thermal Cycler (Bio-Rad, Hercules, CA).

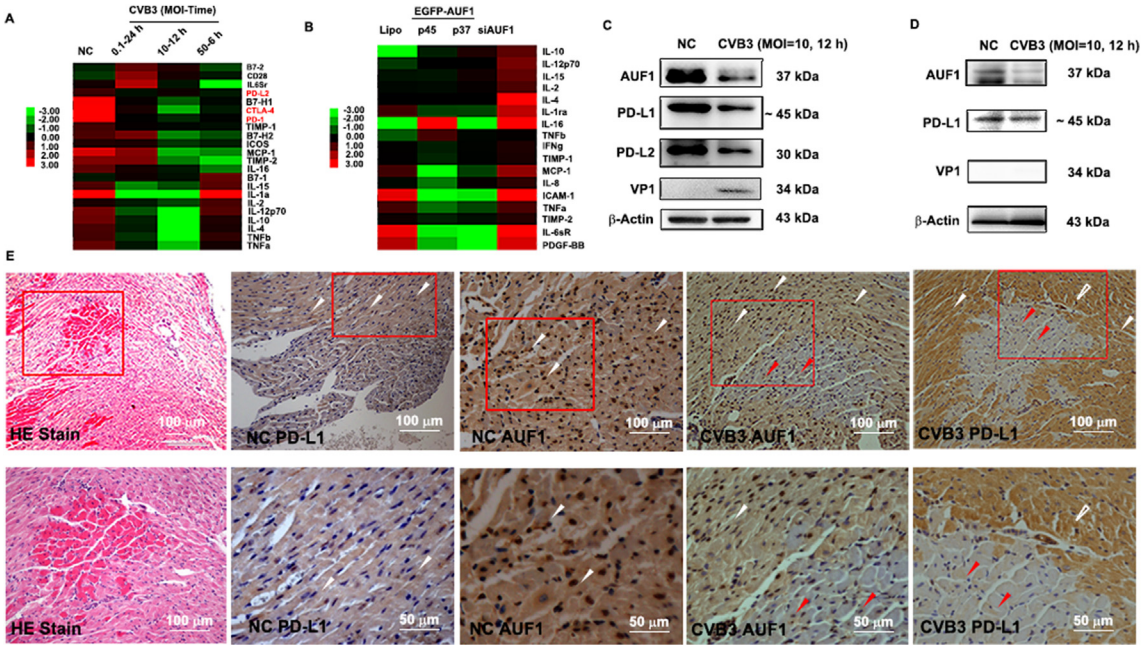

Fig. 1. PD-L1/2 expression decreased in CVB3-infected mouse cardiac myocytes and fibroblasts. (A) The heatmap of the differential expression of various molecules detected by a protein array (QAH-ICM-1). The bars represent the levels of tested proteins in the CVB3-infected cells (MOI = 0.1 at 24 h p.i., MOI = 10 at 12 h p.i., and MOI = 50 at 6 h p.i., respectively) and control cells (NC). (B) The heatmap of the differential expression of cytokines tested with a protein array (QAH-INF-3). The bars represent the cytokine levels in the control cells (Lipo, treated with Lipofectamine 2000 only), in the cells with overexpression of the p45 and p37 isoforms of EGFP-AUF1, and in the cells with AUF1 knockdown. The color gradients from bright green to red represent the levels from low to high expression. (C, D) The expression of AUF1, PD-L1, and PD-L2 in the primary cardiac myocytes (C) and fibroblasts (D) infected with CVB3 (MOI = 10) at 12 h p.i. β-Actin was used as loading control. VP1 was detected to check viral infection. (E) HE staining and IHC staining for the myocardial frozen sections of the suckling Balb/c mice infected with 10^6 pfu of CVB3 for 4–5 days. The typical lesion and staining foci are indicated by red box, and amplified views are showed in the lower panel. White arrow indicates the healthy or non-infected myocardial tissues of the control and the CVB3-infected mice. Red arrow indicates the typical myocardial lesion in the CVB3-infected mice.

The quantitative real-time PCR (RT-qPCR) was performed by using CFX96 Touch (Bio-Rad) according to the protocol recommended by the manufacturer of TB Green *Premix Ex Taq* II (Tli RNaseH Plus) (TaKaRa, Beijing, China). The reaction was carried out in a mixture with a total volume of 20 μl, which included 10 μl SYBR Premix Ex *Taq*II (TaKaRa, Beijing, China), 0.8 μl of forward and reverse primers (10 μM), 2 μl cDNA template, and 6.4 μl ddH_2O. Forty amplification cycles were performed as follows: 95 °C for 5 s, 55 °C for 20 s, and 72 °C for 15 s. Data were analyzed with $2^{-\Delta\Delta Ct}$ method described previously (Livak and Schmittgen, 2001). The sequences of the primers used are listed in Supplementary Table 2. The remaining *PD-L1/2* mRNAs were calculated to determine their half-lives ($t_{1/2}$, the period for each transcript to reach 50% of their original abundance). Transcript levels were normalized to the abundance of *GAPDH* mRNA.

2.6. Isolation of cardiac myocytes and fibroblasts

Cardiac myocytes and fibroblasts were prepared from neonatal mice within 72 h of birth. The heart was minced into 0.5–1 mm^3 pieces, washed twice with cold D-Hanks' medium and then treated with stepwise enzymatic digestion with 0.1% trypsin and 0.2% collagenase I. The dissociated cells were washed with PBS and adsorbed onto plastic flasks at 37 °C and 5% CO_2 for 2 h for fibroblast attachment. The attached cardiac fibroblasts were then washed and cultured in DMEM supplemented with 10% FBS for 24 h. The remaining non-adherent cells were re-suspended in 10% FBS DMEM/F12 with BrdU (0.1 mmol/L) and inoculated into a new culture flask for 48 h to harvest cardiac myocytes. According to the observation of the beating activity of the cells obtained, more than 95% of the cells were identified as cardiac myocytes.

2.7. Immunohistochemical staining and myocarditis severity evaluation

The heart tissues were collected at day 8 p.i., fixed in 4% paraformaldehyde solution, then sectioned and stained with hematoxylin and eosin (HE). The heart sections were examined by two independent investigators to assess the severity of myocarditis. For immunohistochemical staining (IHC), paraffin-embedded samples were stained with the corresponding primary antibodies (anti-AUF1, Cat# 61193, Abcam; anti-PD-L1, Cat# 66248-1-Ig and anti-PD-L2, Cat# 18251-1-AP, Proteintech, Wuhan, China) according to the manufacturer's protocol. The slides were counterstained with hematoxylin. Images were obtained using a Nikon Eclipse 80i microscope.

2.8. Recombination of mPD-L1-Fc and mPD-L2-Fc fusion proteins and hydrodynamic injection

The plasmids expressing fusion proteins mPD-L1-IgG1 Fc and mPD-L2-IgG1 Fc were constructed based on pCMV3 according to the strategy described previously (Chen, 2004; Deng et al., 2015). The cDNAs encoding the extracellular region of murine PD-L1 and PD-L2 were fused with the CH2-CH3 region of human IgG1, respectively, and inserted to the multiple cloning site of pCMV3. The constructs were verified by sequencing and designated as mPD-L1-Fc and mPD-L2-Fc. A plasmid expressing the CH2-CH3 fragment of IgG1 was also constructed as control. For hydrodynamic injection, the purified plasmids (10 μg/ml) were injected into the tail vein at a volume (ml) of 10% body weight (g) (Li et al., 2012; Liu et al., 1999; Suda and Liu, 2007). At day 3, 5, 7, 14, 21, and 28 p.i., serum was obtained by cutting off tails of the mice, and the concentration of the recombinant protein was detected by ELISA.

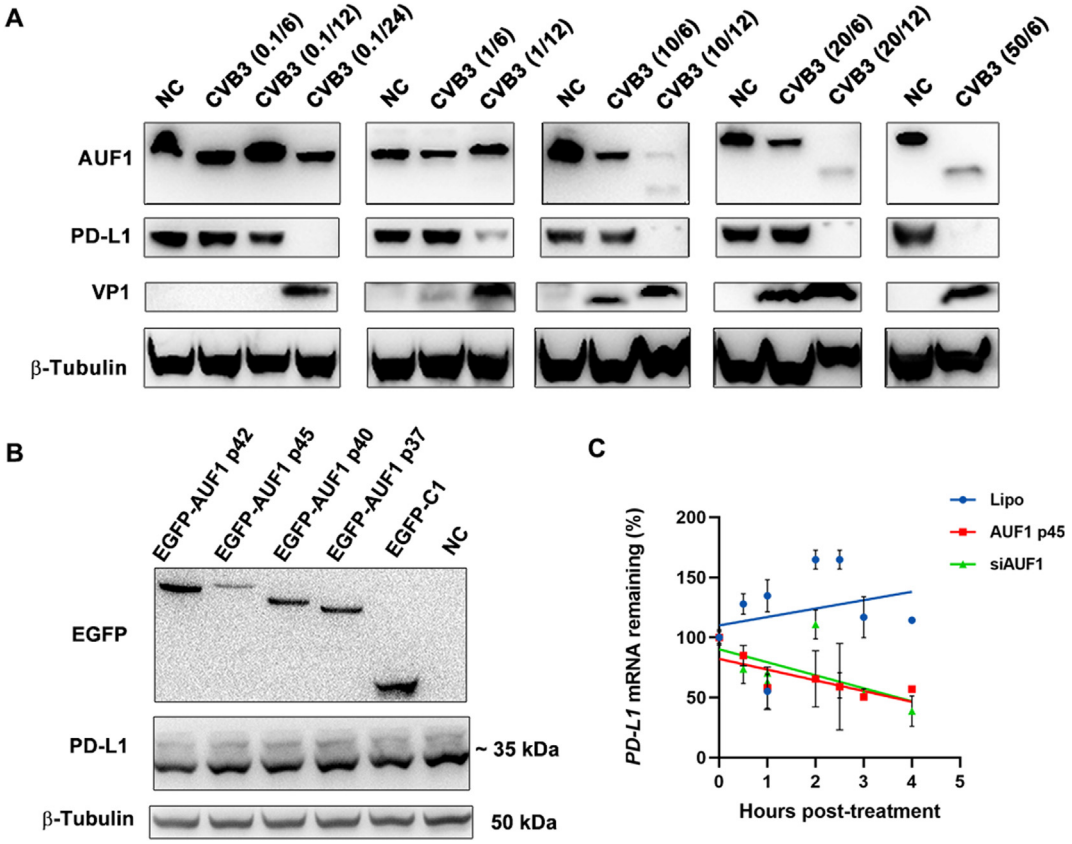

Fig. 2. CVB3-induced AUF1 cleavage affects PD-L1 protein expression, while not *PD-L1* mRNA stability. (A) HeLa cells were infected by CVB3 with various MOIs and time courses. The infected groups are labeled as "CVB3 (MOI/hours of infection)". The expression of AUF1, PD-L1, CVB3 VP1 were detected by western blotting. β-Tubulin was used as loading control. (B) The expression of AUF1 and PD-L1 in HeLa cells transfected with EGFP-tagged p45, p42, p40, and p37 isoforms of AUF1 were detected by western blotting. β-Tubulin was used as loading control. (C) The half-life of *PD-L1* mRNA was detected in the cells with AUF1 overexpression (red) or with siAUF1 treatment (green). Actinomycin D (ActD, 10 μg/ml) was added to the medium 30 min before the RNA extraction at 0-h post-treatment. Error bars represent standard deviation (n = 3).

2.9. Bioinformatic analysis

All the bioinformatic analysis was done by R software. R package pheatmap was used for plotting the heatmap in Supplementary Fig. 1. R package limma was used for variation analysis. R package ggfortity was used for principle component analysis in Supplementary Fig. 1. (R version 3.5.3 was used).

3. Results

3.1. The expression of PD-1 ligand is decreased in CVB3-infected cells

Previously, we reported that AUF1 can be cleaved by CVB3 $3C^{pro}$ (Wong et al., 2013). To focus on the changes brought by AUF1 cleavage, HeLa cells were transfected with plasmids expressing EGFP-tagged p45 and p37 isoforms of AUF1, and with siAUF1, respectively. The cytokine expression profiles were detected with a protein array (QAH-INF-3 Array, Raybiotech, Guangzhuo, China) 24 h post-transfection. As shown in Fig. 1B, the cytokine expression was mostly down-regulated in the cells with AUF1 overexpression, while up-regulated in the cells with AUF1 knockdown. The list of the cytokines, which were differentially expressed in the cells with AUF1 overexpression or knockdown (Fig. 1B) is provided in Supplementary Table 1. According to previous study (Palanisamy et al., 2008), this might be the consequence that AUF1 regulates mRNA stability through binding with AU-rich elements in the mRNA's 3′UTR. However, we cannot rule out another possibility - the potential effects of AUF1 on other pathways, e.g., immune checkpoint molecules that relate to the activation or inhibition of T cells.

To evaluate the effects of AUF1 during CVB3 infection, we first detected the expression of cytokines and immune checkpoint molecules (Supplementary Table 1) in the CVB3-infected HeLa cells with a protein array (QAH-ICM-1 Array, Raybiotech). Interestingly, as shown in Fig. 1A, the expression of these costimulatory molecules including CD28 moderately increased in the cells infected with a small dose of CVB3 (multiplicity of infection (MOI) = 0.1) for 24 h, while the expression of the inhibitory costimulatory molecules, including PD-L1, PD-L2, and CTLA-4, significantly decreased in the cells infected with higher doses of CVB3 (MOI = 10 and 50). The level changes of both CVB3 infection and AUF1 significantly affected the expression of inhibitory costimulatory molecules such as PD-1, PD-1 ligands, and CTLA-4 (Supplementary Fig. 1A).

To verify these findings, primary cardiac myocytes isolated from suckling Balb/c mice were infected with CVB3 (MOI = 10). As shown in Fig. 1C, the levels of PD-L1 and PD-L2 decreased at 12 h post-infection (p.i.). The level of AUF1 was also simultaneously decreased. We also verified it under *in vivo* condition. About three-week-old Balb/c mice were inoculated with CVB3 (10^6 pfu) intraperitoneally. The myocardial tissues were collected and observed with HE staining and IHC assay at 4–5 days p.i. As shown in Fig. 1E, typical inflammatory lesions in the myocardial tissues confirmed the CVB3 infection occurred in HE staining sections (left, red box). Compared to the normal controls (NC AUF1), AUF1 expression dramatically reduced in the infected myocardial tissues (CVB3 AUF1). The translocation of AUF1 from the nucleus to cytoplasm could be observed in the lesions (red arrows), in contrast, AUF1 mostly located in the nucleus in the adjacent non-

infected tissues (white arrows). Coincidentally, PD-L1 expression was also significantly reduced in the lesions (CVB3 PD-L1, red arrows), and elevated in adjacent non-infected tissues (CVB3 PD-L1, white arrows). We further examined the expression of PD-L1 in the CVB3-infected cardiac fibroblasts. Although the level of AUF1 significantly reduced, PD-L1 level did not show an obvious decrease in the CVB3-infected fibroblasts (Fig. 1D). In addition, bioinformatic analysis showed that under the conditions of overexpression or knockdown of AUF1, along with CVB3 infection (Supplementary Fig. 1B and 1C), PD-1 and PD-L2 were significantly regulated based on principle component analysis (PCA).

Taken together, it seems that the expression of PD-1 and its ligands can be heavily affected by CVB3 infection and the consequent AUF1 degradation.

3.2. The abnormal expression of PD-1 ligands during CVB3 infection is related to AUF1 degradation

A series of protein turnovers are regulated by AUF1 through its binding to the AU-rich elements (AREs) in the 3′UTR of the mRNAs. To explore the connection among PD-1 ligands, AUF1, and CVB3 infection, HeLa cells were infected with various doses of CVB3 for 6–24 h. We found that AUF1 level was significantly decreased in the cells with high MOI (10, 20, 50) of CVB3 and long period of infection (12 and 24 h p.i.) (Fig. 2A). This is consistent with our previous report, which demonstrated that AUF1 was degraded by the protease $3C^{pro}$ of CVB (Wong et al., 2013). Interestingly, PD-L1 expression was also significantly decreased in the infected cells (Fig. 2A). The synchronized loss of AUF1 and PD-L1 implies a possible connection between them, although there was no obvious change of PD-L1 expression in the cells expressing EGFP-tagged AUF1 isoforms (p45, p42, p40, and p37) (Fig. 2B).

We further observed the stability of *PD-L1* mRNA in the cells with AUF1 p45 or siAUF1 by testing the half-life of *PD-L1* mRNA (Fig. 2C). Compared to the control cells (transfected with pEGFP-C1) (Fig. S2), *PD-L1* mRNA degradation kept the same rates in the cells with overexpression or knockdown of AUF1. The half-life data suggest that *PD-L1* mRNA might not be solely modulated by AUF1. It is likely that there are other RNA-binding proteins that also participate in the modulation of the stability of *PD-L1* mRNA.

On the other hand, our data indicated that AUF1 directly influenced the stability of *PD-L2* mRNA. PD-L2 expression was significantly increased in the cells with AUF1 overexpression (Fig. 3A), while it was reduced in the cells with siAUF1 (Fig. 3A). The half-life of *PD-L2* mRNA in the cells transfected with AUF1 p45 and p37 isoforms showed a slower degradation rate than that in the control cells (EGFP-C1) (Fig. 3B). The half-life of *PD-L2* mRNA in the cells with AUF1 knockdown was not detectable probably due to the low baseline at the initial time point (when ActD was added). Therefore, *PD-L2* mRNA abundance in the cells with AUF1 overexpression or AUF1 knockdown for 48 h was detected. Indeed, the abundance of *PD-L2* mRNA significantly decreased in siAUF1-treated cells. Conversely, it increased in the cells overexpressing AUF1 p45 (Fig. 3C). These findings demonstrate that AUF1 not only stabilizes *PD-L2* mRNA but also facilitates its transcription. Loss of AUF1 could destabilize *PD-L2* mRNA, leading to the reduced PD-L2 expression.

3.3. PD-1 ligands suppress the inflammatory infiltration caused by CVB3 infection

To evaluate the outcome of reduced PD-1 ligands expression in the myocardial pathogenesis of CVB3 infection, two recombinant CVB3 variants, which carried the mouse genes of PD-L1 and PD-L2, respectively, were constructed and designated as rCVB3-L1 and rCVB3-L2 (Fig. 4A). Both rCVB3-L1 and rCVB3-L2 could infect cells and be stably passaged. The mouse PD-L1 and PD-L2 could be expressed in the HeLa cells infected with the variants (Fig. 4C).

Upon inoculating Balb/c mice with EGFP-CVB3, rCVB3-L1, and rCVB3-L2 (10^6 pfu, i.p.), respectively, the myocardial tissues were collected at the 8-day post-infection. HE staining showed that both rCVB3-L1 and rCVB3-L2 could cause typical inflammatory injury in the myocardial tissues of the infected mice (Fig. 4B). Both rCVB3-L1 and rCVB3-L2 exhibited the viral replication levels which are similar to that of EGFP-CVB3 (Fig. 4D, no significant difference was found by Student's *t* test). However, the inflammatory infiltration induced by the rCVB3-L1/L2 variants was significantly alleviate compared to that of the EGFP-CVB3 (Fig. 4E).

3.4. PD-L1 Ig treatment alleviates the inflammatory injury caused CVB3 infection

To further identify the role of the PD-1 pathway in the pathogenesis of CVB infection, a fusion protein of the extracellular region of murine PD-L1 or PD-L2 and the CH2-CH3 region of human IgG1 Fc fragment was used in this study (designed as mPD-L1-Fc and mPD-L2-Fc), respectively. The recombinant plasmids and a control plasmid were given to Balb/c mice through hydrodynamic injection, respectively (Deng et al., 2015; Flies et al., 2011; Li et al., 2012) (Fig. 5A). Sera were collected and examined at day 0, 3, 5, 7, 14, 21, and 28 post-injection.

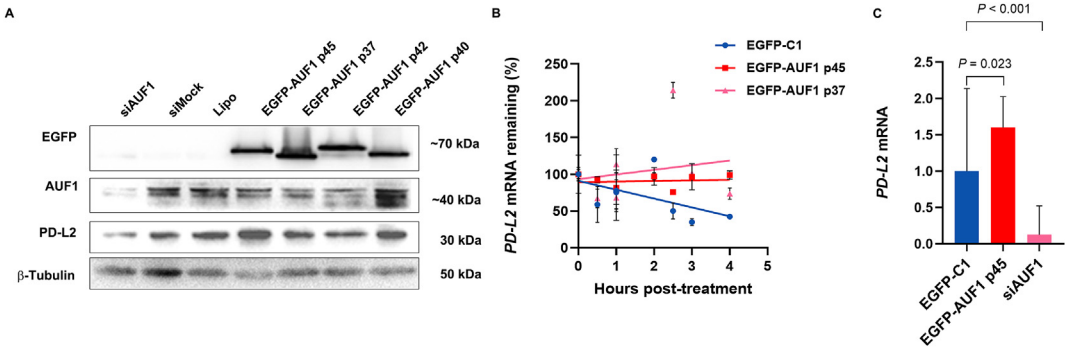

Fig. 3. CVB3-induced AUF1 cleavage affects the expression, mRNA stability, and transcription of PD-L2. (A) HeLa cells were transfected with the EGFP-tagged p45, p42, p40, and p37 isoforms of AUF1, siAUF1, and siMock. At 24 h (for the cells with EGFP-AUF1 plasmid) or 48 h (for the cells with siRNA) post-transfection, the expression of AUF1 and PD-L2 was detected by western blotting. β-Tubulin was used as loading control. (B) To examine the stability of *PD-L2* mRNA, the remaining *PD-L2* mRNA abundance was detected in the cells with overexpression of AUF1 p45 (longest isoform) (red) or p37 (shortest isoform) (pink). ActD (10 μg/ml) was added to terminate the transcription 30 min ahead the RNA extraction at 0-h post-treatment. Error bars represent standard deviation ($n = 3$). (C) *PD-L2* mRNA levels at 24 h post-transfection of EGFP-AUF1 p45 and 48 h post-transfection of siAUF1 were detected by RT-qPCR. GAPDH mRNA was employed as internal reference. A plasmid expressing EGFP only was transfected as normalization control (EGFP-C1). Error bars represent standard deviation ($n = 3$). Student's *t* test was used for the statistical analysis.

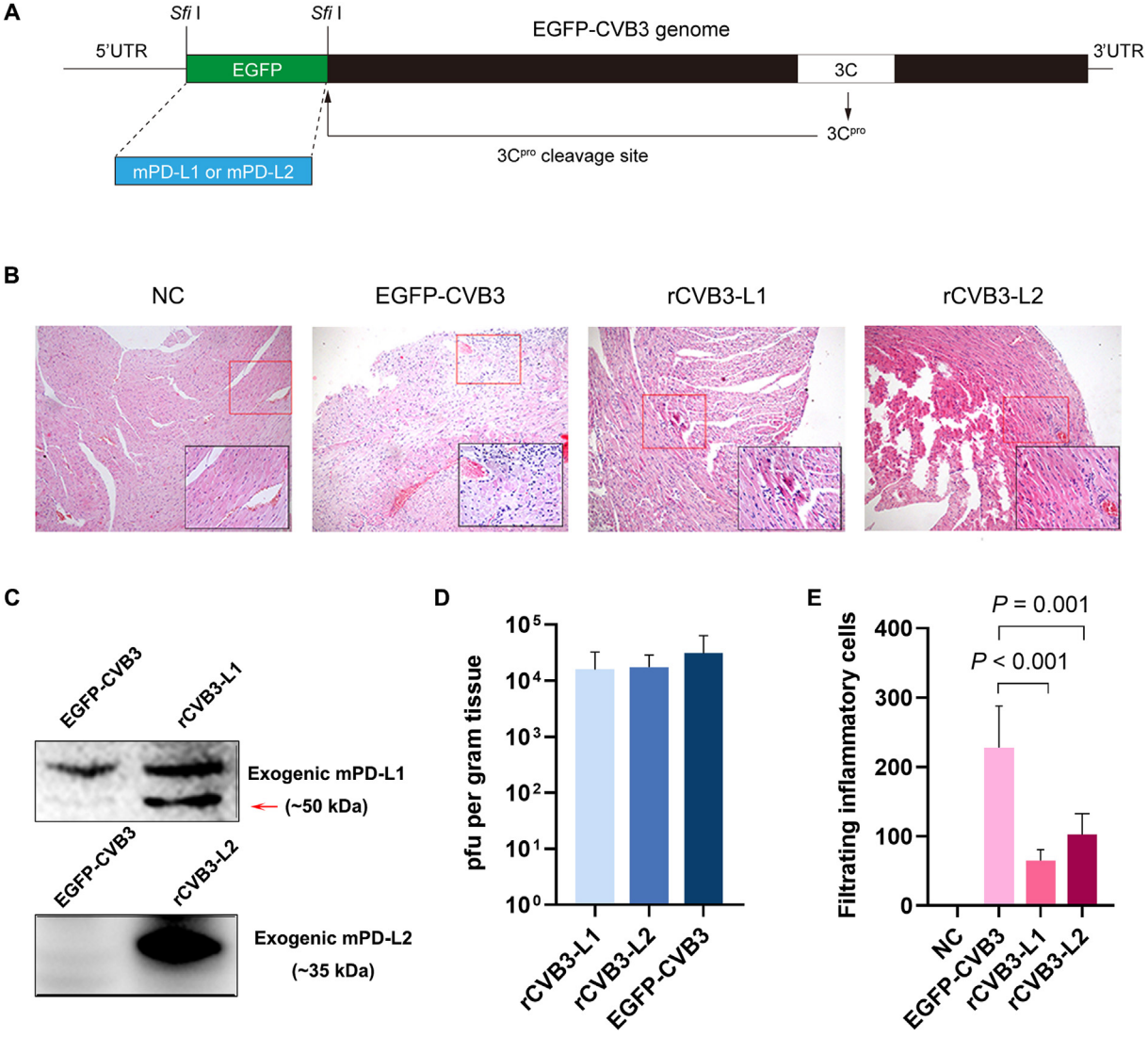

Fig. 4. PD-L1/2-expressing CVB3 variants alleviate the inflammatory infiltration in the myocardial tissue caused by CVB3 infection. (A) A schematic diagram for the construction of CVB3 variants, rCVB3-L1 and rCVB3-L2, which expressed mouse PD-L1 and PD-L2, respectively. The EGFP-coding sequence was replaced by the coding sequence of PD-L1 and PD-L2, respectively. A CVB3 $3C^{pro}$ cleavage site was designed in the beginning of CVB3 open reading frame, which enables PD-L1 and PD-L2 separating from the viral proteins and secures the maturation and assembly of the viral progeny proteins. (B) HE staining of the inflammatory infiltration and injury in the myocardial tissues of the suckling Balb/c mice infected by 10^6 pfu of rCVB3-L1, rCVB3-L2, and EGFP-CVB3, respectively. An amplified view of the red area is shown at the lower right corner (black box). (C) The expression of PD-L1 and PD-L2 in the cells infected with rCVB3-L1, rCVB3-L2, and EGFP-CVB3, respectively, was examined by Western blotting. (D) Titers of rCVB3-L1 and rCVB3-L2 compared to EGFP-CVB3 were detected by $TCID_{50}$ assay. Pfu per gram tissue was calculated. (E) The infiltrating inflammatory cells in the EGFP-CVB3-, rCVB3-L1-, and rCVB3-L2-infected cells were counted in the sections with HE staining. For each group, six views at 200× magnification were randomly selected and the number of infiltrating inflammatory cells (number per mm^2) was counted by two investigators in double-blind way. Student's *t* test was used for statistical analysis. Error bars represent standard deviation ($n = 6$).

Serum mPD-L1-Fc and mPD-L2-Fc in the Balb/c mice reached the peak levels at day 7 post-injection (Fig. 5B and 5C) and were maintained for approximately one week.

According to the preliminary test, we decided to inoculate the mice with CVB3 (10^6 pfu) intraperitoneally at day 5 post-injection of the fusion plasmids and harvested at day 12 post-injection (Fig. 5A, red arrows). The viral replication levels of mPD-L1/2-Fc treated groups were significantly reduced compared to that of control group (Fig. 5E). Compared with the control mice, increased apoptosis of the splenic lymphocytes was observed in the PD-L1-Fc-expressing mice (Fig. 5G and Supplementary Fig. 3). The myocardial injury also reduced significantly in the mPD-L1-Fc plasmid inoculated mice observed by HE staining (Fig. 5D and F). However, there was no obvious difference in the splenic lymphocyte apoptosis and the inflammatory infiltration in heart between the control and mPD-L2-Fc inoculated mice (Figs. 5D, 5F, 5G and Supplementary Fig. 3). Our findings suggest that PD-L1 may play a protective role in CVB infection. The decrease of PD-1 ligand expression during CVB infection may counteract its protection and lead to a severe injury in the heart.

4. Discussion

T cells play a vital role in the adaptive immune response. T cell-mediated cytotoxicity is the most effective mechanism for virus clearance (Chang and Laimins, 2000). T cell activation requires two major signals: one is the signal that TCR recognizes a peptide - MHC complex presented by APCs; another is the signal provided by costimulatory molecules (Liu et al., 2017). Adaptive immune response to defend the host or maintain auto-tolerance is determined by the balance of positive and negative signals from costimulatory molecules (Bahrami et al.,

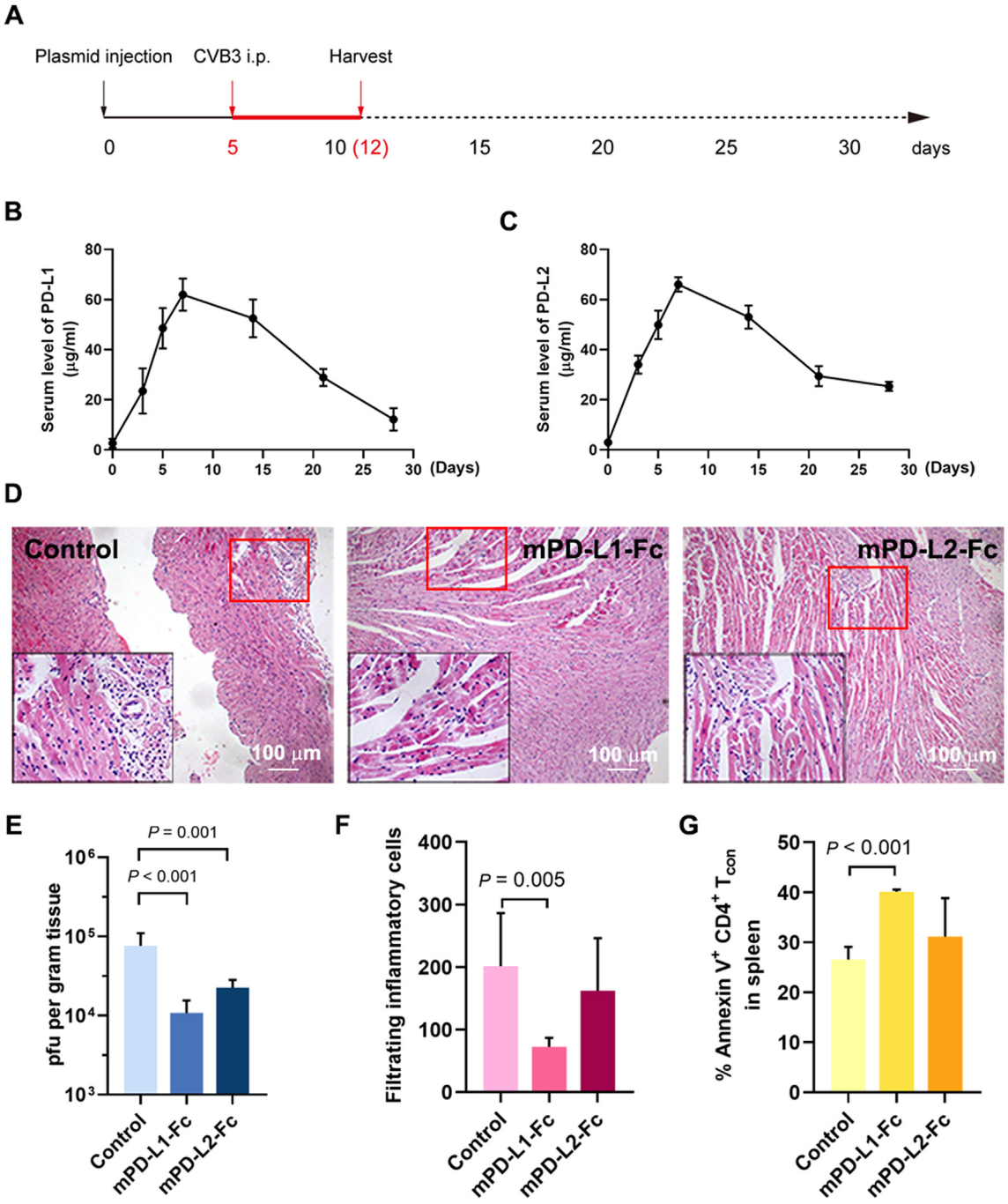

Fig. 5. PD-L1/2-Fc treatment increases the apoptosis of proliferating lymphocytes and decreases the inflammatory infiltration. (A) A diagram for the plasmid injection and virus infection. The plasmids expressing mPD-L1-Fc, mPD-L2-Fc, and IgG1 Fc (as control) were injected to tail veins in suckling Balb/c mice at day 0. The sera were collected in every five days for testing the serum level of PD-L1-Fc and PD-L2-Fc until day 28. According to serum test, the EGFP-CVB3 was intraperitoneally inoculated at day 5 and the mice were sacrificed at day 12 for pathological detection (red line). (B, C) The serum levels of PD-L1-Fc and PD-L2-Fc detected by ELISA. (D) The inflammatory infiltration in the mice with Fc-, mPD-L1-Fc-, and mPD-L2-Fc-expressing plasmids examined by HE staining. An amplified view (400×) is shown at left lower corner. (E) The viral titer per gram tissue from the mice with treatment of mPD-L1-Fc, mPD-L2-Fc, and Fc only, respectively, was calculated by TCID50 assay. (F) The average number of infiltrating inflammatory cells (number per mm^2) in the myocardial tissue was counted in the section with HE staining under 200× magnification. (E) The splenic lymphocyte percentage in the mice with various treatments was detected by flow cytometry. The percentage of Annexin V^+ $CD4^+$ Tcon cells was analyzed. The error bars represent standard deviation ($n = 4$). Student's t test was used for statistical analysis.

2014; Liu et al., 2017). During viral infection, viruses have to evade the host's defense mechanisms, including innate and adaptive immunes. Accumulated data reveal that viruses can block Toll-like receptor and interferon pathways by down-regulating or simply degrading certain key players in these pathways (Huang et al., 2015; Lind et al., 2016; Mukherjee et al., 2011). Presently, it is unclear whether virus circumvents the host's immune response through manipulating costimulatory molecules.

CVB is the major pathogen of human myocarditis and dilated cardiomyopathy. CVB infection induces the host's antiviral immune response, which, conversely, causes inflammatory infiltration and injury (Palanisamy et al., 2008; Wong et al., 2013). In this study, we attempted to evaluate the role of negative costimulatory molecules - PD-1 ligands in the pathogenesis of CVB. We demonstrated that CVB3

infection caused a decreased expression of PD-1 ligands. The decrease of PD-1 ligands expression was partly due to the cleavage of AUF1 by CVB3 protease $3C^{pro}$. Supplementation of PD-1 ligands could greatly improve the inflammatory infiltration in the myocardial tissues of CVB3-infected mice. Overall, suppressing the expression of PD-1 ligands contributes to the pathogenic mechanisms of CVB-related myocarditis. This study implies that PD-1 ligands could be used as protective agents for the therapy of viral myocarditis.

So far, only a few studies paid attention to the relation between CVB infection and PD1 pathway. Seko Y et al. (Filippi et al., 2009; Seko et al., 2007) reported previously that CVB3 infection strongly increased PD-L1 levels in mice cardiac myocytes. Filippi CM et al. (Filippi et al., 2009; Seko et al., 2007) also reported that PD-L1 level increased transiently on lymphoid cells in the pancreas and spleen of non-obese diabetic (NOD) mice infected with CVB3. It seems that there is an inconsistence between our study and these reports. However, after checking these reports carefully, we conclude that there is no conflict among these studies. Our IHC data show that the decreased PD-1 ligand expression predominantly occurred in infection lesion of the myocardial tissue (Fig. 1E). However, in the adjacent "healthy" tissue, PD-L1 expression was actually increased, which was even higher than that in NC mice (Fig. 1E, NC PD-L1). Under *in vitro* condition, the expression of PD-1 ligands was consistently down-regulated in the isolated primary cardiomyocytes and cardiac fibroblasts infected with CVB3 (Fig. 1Cand D). A similar tendency was also observed in HeLa cells (Fig. 2A). The *in vitro* evidence supported our *in vivo* observation. Therefore, we postulate that it is very likely that the global expression of PD-L1 is elevated in the entire cardiac tissue of the infected mouse.

It is unknown why PD-1 ligands expression reduced in the CVB3-infected cells. Previously, we revealed that AUF1 can be degraded by CVB protease $3C^{pro}$ (Wong et al., 2013). AUF1 degradation relieves its negative effect on the stability of CVB genomic RNA, through which CVB protects itself and successfully replicates in the host cells (Wong et al., 2013). Recently, AUF1 has been reported to be a double-edged sword for mRNA stability. In most cases, AUF1 promotes the degradation of mRNAs, while in some cases, AUF1 can also stabilize mRNAs (Palanisamy et al., 2008; Sarkar et al., 2008). Recent studies showed that AUF1 can degrade the mRNAs of various inflammatory cytokines, as long as their mRNAs contain the AREs in the 3′UTRs (DeMaria and Brewer, 1996). Based on our data of cytokine array, overexpression or knockdown of AUF1 could affect the expression of many cytokines and PD-1 ligands (Fig. 1B). AUF1 could stabilize *PD-L2* mRNA (Fig. 3B and C), but it seems that AUF1 did not affect the half-life of *PD-L1* mRNA (Fig. 2B and C). Probably, there are other RNA-binding proteins participating in the modulation of PD-L1 expression. For example, oncogenic RAS signaling was found to be able to upregulate PD-L1 expression through tristetraprolin (TTP), an AU-rich element-binding protein, in tumor cells (Coelho et al., 2017). TTP can stabilize *PD-L1* mRNA (Coelho et al., 2017). Therefore, we concluded that CVB3 could manipulate PD-1 ligands expression, partially due to virus-induced AUF1 degradation. Further study is needed to elucidate the mechanism for the aberrant PD-L1 expression during CVB infection.

T cells orchestrate adaptive immune responses to defend against pathogens while simultaneously avoiding self-reactivity (Hisaeda et al., 2008). The costimulatory molecules expressed on the antigen-presenting cells can interact with T cells. The interaction between T cells and the costimulatory molecules, along with the antigen-specific signals, is crucial for the activation of lymphocytes (Chapoval et al., 2001; Chen, 2004). There is a complex network of stimulatory and inhibitory receptors as well as ligands expressed on T cells (Podojil et al., 2018; van der Vegt et al., 2007). The balance between the stimulatory and inhibitory costimulatory signals determines the initiation, occurrence rate and development of autoimmunity (Chapoval et al., 2001; Montufar-Solis et al., 2007). As an inhibitory costimulatory molecule, compared with CD28, CTLA-4 has greater affinity and avidity for CD80 and CD86, thus enabling it to outcompete CD28 for these ligands. In addition to CTLA-4, PD-1, BTLA, and TIM-3 are newly discovered inhibitory costimulators (Frisancho-Kiss et al., 2007; Su et al., 2016).

PD-1 is critical in the adaptive immune, including humoral and cellular immune responses. PD-1 exerts distinct independent effects during different phases of T cell responses, including regulating the threshold for T cell activation, downregulating T cell proliferation, and inducing apoptosis in activated T cells (Patsoukis et al., 2015). It has been reported that CVB infection suppresses the virus-specific $CD8^+$ T cell response (Lin et al., 2009; Vossen et al., 2002). However, even with the suppression on $CD8^+$ T cell response, lethal inflammation is still frequently developed in the myocardium during the acute phase of CVB infection. According to our data, the decrease of PD-1 ligands may facilitate the inflammatory response during CVB infection. Under *in vivo* condition, supplementing PD-L1/2 by rCVB3-L1/2, two recombinant CVB3 variants, showed a high efficiency of relieving the infiltration of inflammatory cells and structural destructions in the heart tissue (Fig. 4). Furthermore, PD-L1/2-Ig expressing plasmids treatment showed an obvious reduction in inflammatory cell infiltration (Fig. 5). Overall, our work illustrated the potential therapeutic role of PD1 and its ligands against the direct injury and autoimmune response induced by CVB infection. A putative mechanism about the interaction between CVB infection and PD-1 ligands is plotted as Fig. 6.

Besides the potential role of PD-1 for the prevention and treatment of viral infection, PD-1 also shows contribution in targeting therapy of tumors. PD-1 is ligated on T cells through ligands expressed on tumor tissue, normal tissue or virus-infected lesions. This ligation inhibits ZAP70 phosphorylation and its association with CD3ζ (Sheppard et al., 2004) to prevent effector T cell generation and expansion and to maintain effective peripheral tolerance. PD-L1 is expressed widely on macrophages, dendritic cells (DCs), T cells, as well as some non-hematopoietic cells and tissues, including various solid tumor cells (Keir et al., 2008). Therapeutic targeting of the PD-1/PD-L1 pathway with blocking monoclonal antibodies has resulted in the successful enhancement of T cell immunity against various solid tumors. The expression of PD-L2, a new B7 family member discovered in 2001, is relatively restricted to dendritic cells and macrophages stimulated with IFN-γ, GM-CSF, or IL-4 (Yamazaki et al., 2002), while its expression on nonimmune cells is closely related to the local microenvironment. Engagement of PD-1 by PD-L2 dramatically inhibits B7-CD28 signaling and cytokine secretion by $CD4^+$ T cells (Latchman et al., 2001). It has also been reported that PD-L2 expression in solid tumor cells predicts poor prognosis (Shin et al., 2016).

In summary, based on the present study, CVB infection reduces PD-1 ligand expression, partially due to the degradation of AUF1 related with

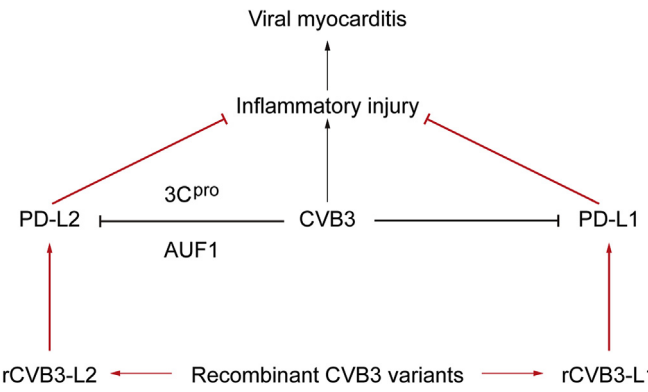

Fig. 6. A putative mechanism for the role of PD-1 ligands in CVB infection. The CVB3 infection decreases the level of PD-L1/2 by degrading AUF1 through its protease $3C^{pro}$. Treatment with PD-L1/2 by the CVB3 variants rCVB3-L1 and rCVB3-L2, or by the plasmids that express mPD-L1-Fc and mPD-L2-Fc suggests that PD-L1/2 can negatively modulate the inflammatory response caused by CVB3 infection and alleviate the inflammatory injury in the myocardial tissue during CVB3 infection.

the enzymatic cleavage by viral protease $3C^{pro}$. Addition of PD-L1 and PD-L2 can dramatically relieve the inflammatory infiltration and injury in the heart muscles caused by CVB infection. PD-1 pathway may be a potential immunotherapeutic target for CVB infection.

Author contributions

Chen S and Zhong ZH designed the study, Wang TY, Chen S, Wang XQ, Huang YK and Anita Chaulagain performed the experiments, Chen S, Wang TY, Zhong ZH and Zhao WR wrote the manuscript, and Chen S, Wang TY, Qiu JF, Wang XQ, Lin LX and Wang Y analyzed the data. Zhong ZH, Zhao WR, Wang W provided the professional consulting support.

Conflict of Interest

The authors declared that they have no competing interests.

Acknowledgments

The study was supported by National Natural Science foundation of China (NSFC) grants to Wang TY (31300144), Zhao WR. (81672007), Zhong ZH (81571999, 81871652), Wang Y (81772188), University Nursing Program for Young Scholars with Creative Talents in Heilongjiang Province to Chen S (UNPYSCT-2018053) and Wang TY (UNPYSCT-2016044), Heilongjiang Province Graduate Innovation Research Grant to Wang TY (YJSCX2015-4HYD) and Fei YR (YJSCX2017-9HYD), and China Scholarship Council Doctoral Scholarship to Wang XQ (201608230108). We thank the technique assistance by Wu Lien-Teh Institution, and Heilongjiang Province Key Laboratory of Infection and Immunology, Harbin Medical University.

Appendix A. Supplementary data

Supplementary data to this article can be found online at https://doi.org/10.1016/j.antiviral.2019.03.007.

References

Bahrami, A.A., Ghaemi, A., Tabarraei, A., Sajadian, A., Gorji, A., Soleimanjahi, H., 2014. DNA vaccine encoding HPV-16 E7 with mutation in L-Y-C-Y-E pRb-binding motif induces potent anti-tumor responses in mice. J. Virol. Methods 206, 12–18.
Chang, Y.E., Laimins, L.A., 2000. Microarray analysis identifies interferon-inducible genes and Stat-1 as major transcriptional targets of human papillomavirus type 31. J. Virol. 74, 4174–4182.
Chapoval, A.I., Ni, J., Lau, J.S., Wilcox, R.A., Flies, D.B., Liu, D., Dong, H., Sica, G.L., Zhu, G., Tamada, K., Chen, L., 2001. B7-H3: a costimulatory molecule for T cell activation and IFN-gamma production. Nat. Immunol. 2, 269–274.
Chen, L., 2004. Co-inhibitory molecules of the B7-CD28 family in the control of T-cell immunity. Nat. Rev. Immunol. 4, 336–347.
Cheung, P., Zhang, M., Yuan, J., Chau, D., Yanagawa, B., McManus, B., Yang, D., 2002. Specific interactions of HeLa cell proteins with Coxsackievirus B3 RNA: La autoantigen binds differentially to multiple sites within the 5' untranslated region. Virus Res. 90, 23–36.
Coelho, M.A., de Carne Trecesson, S., Rana, S., Zecchin, D., Moore, C., Molina-Arcas, M., East, P., Spencer-Dene, B., Nye, E., Barnouin, K., Snijders, A.P., Lai, W.S., Blackshear, P.J., Downward, J., 2017. Oncogenic RAS signaling promotes tumor immunoresistance by stabilizing PD-L1 mRNA. Immunity 47, 1083–1099 e1086.
DeMaria, C.T., Brewer, G., 1996. AUF1 binding affinity to A+U-rich elements correlates with rapid mRNA degradation. J. Biol. Chem. 271, 12179–12184.
Deng, R., Cassady, K., Li, X., Yao, S., Zhang, M., Racine, J., Lin, J., Chen, L., Zeng, D., 2015. B7H1/CD80 interaction augments PD-1-dependent T cell apoptosis and ameliorates graft-versus-host disease. J. Immunol. 194, 560–574.
Duncan, B.W., Bohn, D.J., Atz, A.M., French, J.W., Laussen, P.C., Wessel, D.L., 2001. Mechanical circulatory support for the treatment of children with acute fulminant myocarditis. J. Thorac. Cardiovasc. Surg. 122, 440–448.
Durani, Y., Giordano, K., Goudie, B.W., 2010. Myocarditis and pericarditis in children. Pediatr. Clin. 57, 1281–1303.
Fairweather, D., Frisancho-Kiss, S., Rose, N.R., 2005. Viruses as adjuvants for autoimmunity: evidence from Coxsackievirus-induced myocarditis. Rev. Med. Virol. 15, 17–27.
Fairweather, D., Rose, N.R., 2007. Coxsackievirus-induced myocarditis in mice: a model of autoimmune disease for studying immunotoxicity. Methods 41, 118–122.
Fairweather, D., Stafford, K.A., Sung, Y.K., 2012. Update on coxsackievirus B3 myocarditis. Curr. Opin. Rheumatol. 24, 401–407.
Filippi, C.M., Estes, E.A., Oldham, J.E., von Herrath, M.G., 2009. Immunoregulatory mechanisms triggered by viral infections protect from type 1 diabetes in mice. J. Clin. Investig. 119, 1515–1523.
Flies, D.B., Sandler, B.J., Sznol, M., Chen, L., 2011. Blockade of the B7-H1/PD-1 pathway for cancer immunotherapy. Yale J. Biol. Med. 84, 409–421.
Frisancho-Kiss, S., Davis, S.E., Nyland, J.F., Frisancho, J.A., Cihakova, D., Barrett, M.A., Rose, N.R., Fairweather, D., 2007. Cutting edge: cross-regulation by TLR4 and T cell Ig mucin-3 determines sex differences in inflammatory heart disease. J. Immunol. 178, 6710–6714.
Garmaroudi, F.S., Marchant, D., Hendry, R., Luo, H., Yang, D., Ye, X., Shi, J., McManus, B.M., 2015. Coxsackievirus B3 replication and pathogenesis. Future Microbiol. 10, 629–653.
Guo, G., Li, H., Cao, D., Chen, Y., 2014. The development of endometrial hyperplasia in aged PD-1-deficient female mice. Diagn. Pathol. 9, 97.
Heymans, S., Eriksson, U., Lehtonen, J., Cooper Jr., L.T., 2016. The quest for new approaches in myocarditis and inflammatory cardiomyopathy. J. Am. Coll. Cardiol. 68, 2348–2364.
Hisaeda, H., Tetsutani, K., Imai, T., Moriya, C., Tu, L., Hamano, S., Duan, X., Chou, B., Ishida, H., Aramaki, A., Shen, J., Ishii, K.J., Coban, C., Akira, S., Takeda, K., Yasutomo, K., Torii, M., Himeno, K., 2008. Malaria parasites require TLR9 signaling for immune evasion by activating regulatory T cells. J. Immunol. 180, 2496–2503.
Hong, X., Wang, X., Wang, T., Zhang, X., 2018. Correlation of T Cell immunoglobulin and ITIM domain (TIGIT) and programmed death 1 (PD-1) with clinicopathological characteristics of renal cell carcinoma may indicate potential targets for treatment. Med. Sci. Mon. Int. Med. J. Exp. Clin. Res. 24, 6861–6872.
Huang, L., Liu, Q., Zhang, L., Zhang, Q., Hu, L., Li, C., Wang, S., Li, J., Zhang, Y., Yu, H., Wang, Y., Zhong, Z., Xiong, T., Xia, X., Wang, X., Yu, L., Deng, G., Cai, X., Cui, S., Weng, C., 2015. Encephalomyocarditis virus 3C protease relieves TRAF family member-associated NF-kappaB activator (TANK) inhibitory effect on TRAF6-mediated NF-kappaB signaling through cleavage of tank. J. Biol. Chem. 290, 27618–27632.
Huang, X., Yang, Y., 2009. Innate immune recognition of viruses and viral vectors. Hum. Gene Ther. 20, 293–301.
Jubelt, B., Lipton, H.L., 2014. Enterovirus/picornavirus infections. Handb. Clin. Neurol. 123, 379–416.
Keir, M.E., Butte, M.J., Freeman, G.J., Sharpe, A.H., 2008. PD-1 and its ligands in tolerance and immunity. Annu. Rev. Immunol. 26, 677–704.
Kim, J.M., Rasmussen, J.P., Rudensky, A.Y., 2007. Regulatory T cells prevent catastrophic autoimmunity throughout the lifespan of mice. Nat. Immunol. 8, 191–197.
Kim, K.S., Hufnagel, G., Chapman, N.M., Tracy, S., 2001. The group B coxsackieviruses and myocarditis. Rev. Med. Virol. 11, 355–368.
Kmieciak, M., Gowda, M., Graham, L., Godder, K., Bear, H.D., Marincola, F.M., Manjili, M.H., 2009. Human T cells express CD25 and Foxp3 upon activation and exhibit effector/memory phenotypes without any regulatory/suppressor function. J. Transl. Med. 7, 89.
Knowlton, K.U., Jeon, E.S., Berkley, N., Wessely, R., Huber, S., 1996. A mutation in the puff region of VP2 attenuates the myocarditic phenotype of an infectious cDNA of the Woodruff variant of coxsackievirus B3. J. Virol. 70, 7811–7818.
Latchman, Y., Wood, C.R., Chernova, T., Chaudhary, D., Borde, M., Chernova, I., Iwai, Y., Long, A.J., Brown, J.A., Nunes, R., Greenfield, E.A., Bourque, K., Boussiotis, V.A., Carter, L.L., Carreno, B.M., Malenkovich, N., Nishimura, H., Okazaki, T., Honjo, T., Sharpe, A.H., Freeman, G.J., 2001. PD-L2 is a second ligand for PD-1 and inhibits T cell activation. Nat. Immunol. 2, 261–268.
Lesokhin, A.M., Ansell, S.M., Armand, P., Scott, E.C., Halwani, A., Gutierrez, M., Millenson, M.M., Cohen, A.D., Schuster, S.J., Lebovic, D., Dhodapkar, M., Avigan, D., Chapuy, B., Ligon, A.H., Freeman, G.J., Rodig, S.J., Cattry, D., Zhu, L., Grosso, J.F., Bradley Garelik, M.B., Shipp, M.A., Borrello, I., Timmerman, J., 2016. Nivolumab in patients with relapsed or refractory hematologic malignancy: preliminary results of a phase ib study. J. Clin. Oncol. 34, 2698–2704.
Li, X., Deng, R., He, W., Liu, C., Wang, M., Young, J., Meng, Z., Du, C., Huang, W., Chen, L., Chen, Y., Martin, P., Forman, S., Zeng, D., 2012. Loss of B7-H1 expression by recipient parenchymal cells leads to expansion of infiltrating donor CD8+ T cells and persistence of graft-versus-host disease. J. Immunol. 188, 724–734.
Liao, Y., Chen, K.H., Dong, X.M., Fang, Y., Li, W.G., Huang, G.Y., Song, W., 2015. A role of pre-mir-10a coding region variant in host susceptibility to coxsackie virus-induced myocarditis. Eur. Rev. Med. Pharmacol. Sci. 19, 3500–3507.
Lin, Y.W., Chang, K.C., Kao, C.M., Chang, S.P., Tung, Y.Y., Chen, S.H., 2009. Lymphocyte and antibody responses reduce enterovirus 71 lethality in mice by decreasing tissue viral loads. J. Virol. 83, 6477–6483.
Lind, K., Svedin, E., Domsgen, E., Kapell, S., Laitinen, O.H., Moll, M., Flodstrom-Tullberg, M., 2016. Coxsackievirus counters the host innate immune response by blocking type III interferon expression. J. Gen. Virol. 97, 1368–1380.
Lipson, E.J., Sharfman, W.H., Drake, C.G., Wollner, I., Taube, J.M., Anders, R.A., Xu, H., Yao, S., Pons, A., Chen, L., Pardoll, D.M., Brahmer, J.R., Topalian, S.L., 2013. Durable cancer regression off-treatment and effective reinduction therapy with an anti-PD-1 antibody. Clin. Cancer Res. 19, 462–468.
Liu, C., Lu, J., Tian, H., Du, W., Zhao, L., Feng, J., Yuan, D., Li, Z., 2017. Increased expression of PD-L1 by the human papillomavirus 16 E7 oncoprotein inhibits anticancer immunity. Mol. Med. Rep. 17, 1063–1070.
Liu, F., Song, Y., Liu, D., 1999. Hydrodynamics-based transfection in animals by systemic administration of plasmid DNA. Gene Ther. 6, 1258–1266.
Livak, K.J., Schmittgen, T.D., 2001. Analysis of relative gene expression data using real-time quantitative PCR and the 2(-Delta Delta C(T)) method. Methods 25, 402–408.
Malenovska, H., 2013. Virus quantitation by transmission electron microscopy, TCID(5)(0), and the role of timing virus harvesting: a case study of three animal viruses. J.

Virol. Methods 191, 136–140.
Marchant, D., Si, X., Luo, H., McManus, B., Yang, D., 2008. The impact of CVB3 infection on host cell biology. Curr. Top. Microbiol. Immunol. 323, 177–198.
Montufar-Solis, D., Wang, H.C., Klein, J.R., 2007. Stimulatory and costimulatory effects of IL-18 directed to different small intestinal CD43 T cell subsets. J. Leukoc. Biol. 82, 1166–1173.
Mukherjee, A., Morosky, S.A., Delorme-Axford, E., Dybdahl-Sissoko, N., Oberste, M.S., Wang, T., Coyne, C.B., 2011. The coxsackievirus B 3C protease cleaves MAVS and TRIF to attenuate host type I interferon and apoptotic signaling. PLoS Pathog. 7, e1001311.
Paiva, B., Azpilikueta, A., Puig, N., Ocio, E.M., Sharma, R., Oyajobi, B.O., Labiano, S., San-Segundo, L., Rodriguez, A., Aires-Mejia, I., Rodriguez, I., Escalante, F., de Coca, A.G., Barez, A., San Miguel, J.F., Melero, I., 2015. PD-L1/PD-1 presence in the tumor microenvironment and activity of PD-1 blockade in multiple myeloma. Leukemia 29, 2110–2113.
Palanisamy, V., Park, N.J., Wang, J., Wong, D.T., 2008. AUF1 and HuR proteins stabilize interleukin-8 mRNA in human saliva. J. Dent. Res. 87, 772–776.
Patsoukis, N., Bardhan, K., Chatterjee, P., Sari, D., Liu, B., Bell, L.N., Karoly, E.D., Freeman, G.J., Petkova, V., Seth, P., Li, L., Boussiotis, V.A., 2015. PD-1 alters T-cell metabolic reprogramming by inhibiting glycolysis and promoting lipolysis and fatty acid oxidation. Nat. Commun. 6, 6692.
Podojil, J.R., Hecht, I., Chiang, M.Y., Vaknin, I., Barbiro, I., Novik, A., Neria, E., Rotman, G., Miller, S.D., 2018. ILDR2-Fc is a novel regulator of immune homeostasis and inducer of antigen-specific immune tolerance. J. Immunol. 200, 2013–2024.
Ray, A., Das, D.S., Song, Y., Richardson, P., Munshi, N.C., Chauhan, D., Anderson, K.C., 2015. Targeting PD1-PDL1 immune checkpoint in plasmacytoid dendritic cell interactions with T cells, natural killer cells and multiple myeloma cells. Leukemia 29, 1441–1444.
Rose, N.R., 2011. Critical cytokine pathways to cardiac inflammation. J. Interferon Cytokine Res. 31, 705–710.
Rose, N.R., 2016. Viral myocarditis. Curr. Opin. Rheumatol. 28, 383–389.
Sarkar, S., Sinsimer, K.S., Foster, R.L., Brewer, G., Pestka, S., 2008. AUF1 isoform-specific regulation of anti-inflammatory IL10 expression in monocytes. J. Interferon Cytokine Res. 28, 679–691.
Seko, Y., Yagita, H., Okumura, K., Azuma, M., Nagai, R., 2007. Roles of programmed death-1 (PD-1)/PD-1 ligands pathway in the development of murine acute myocarditis caused by coxsackievirus B3. Cardiovasc. Res. 75, 158–167.
Sharpe, A.H., Pauken, K.E., 2018. The diverse functions of the PD1 inhibitory pathway. Nat. Rev. Immunol. 18, 153–167.
Sheppard, K.A., Fitz, L.J., Lee, J.M., Benander, C., George, J.A., Wooters, J., Qiu, Y., Jussif, J.M., Carter, L.L., Wood, C.R., Chaudhary, D., 2004. PD-1 inhibits T-cell receptor induced phosphorylation of the ZAP70/CD3zeta signalosome and downstream signaling to PKCtheta. FEBS Lett. 574, 37–41.
Shin, S.J., Jeon, Y.K., Kim, P.J., Cho, Y.M., Koh, J., Chung, D.H., Go, H., 2016. Clinicopathologic analysis of PD-L1 and PD-L2 expression in renal cell carcinoma: association with oncogenic proteins status. Ann. Surg. Oncol. 23, 694–702.
Sponaas, A.M., Moharrami, N.N., Feyzi, E., Standal, T., Holth Rustad, E., Waage, A., Sundan, A., 2015. PDL1 expression on plasma and dendritic cells in myeloma bone marrow suggests benefit of targeted anti PD1-PDL1 therapy. PLoS One 10, e0139867.
Su, N., Yue, Y., Xiong, S., 2016. Monocytic myeloid-derived suppressor cells from females, but not males, alleviate CVB3-induced myocarditis by increasing regulatory and CD4(+)IL-10(+) T cells. Sci. Rep. 6, 22658.
Suda, T., Liu, D., 2007. Hydrodynamic gene delivery: its principles and applications. Mol. Ther. 15, 2063–2069.
Tamura, H., Ishibashi, M., Yamashita, T., Tanosaki, S., Okuyama, N., Kondo, A., Hyodo, H., Shinya, E., Takahashi, H., Dong, H., Tamada, K., Chen, L., Dan, K., Ogata, K., 2013. Marrow stromal cells induce B7-H1 expression on myeloma cells, generating aggressive characteristics in multiple myeloma. Leukemia 27, 464–472.
Tong, L., Lin, L., Zhao, W., Wang, B., Wu, S., Liu, H., Zhong, X., Cui, Y., Gu, H., Zhang, F., Zhong, Z., 2011. Destabilization of coxsackievirus b3 genome integrated with enhanced green fluorescent protein gene. Intervirology 54, 268–275.
van der Vegt, B., de Roos, M.A., Peterse, J.L., Patriarca, C., Hilkens, J., de Bock, G.H., Wesseling, J., 2007. The expression pattern of MUC1 (EMA) is related to tumour characteristics and clinical outcome of invasive ductal breast carcinoma. Histopathology 51, 322–335.
Vossen, M.T., Westerhout, E.M., Soderberg-Naucler, C., Wiertz, E.J., 2002. Viral immune evasion: a masterpiece of evolution. Immunogenetics 54, 527–542.
Wong, J., Si, X., Angeles, A., Zhang, J., Shi, J., Fung, G., Jagdeo, J., Wang, T., Zhong, Z., Jan, E., Luo, H., 2013. Cytoplasmic redistribution and cleavage of AUF1 during coxsackievirus infection enhance the stability of its viral genome. FASEB J. 27, 2777–2787.
Woodruff, J.F., 1980. Viral myocarditis. A review. Am. J. Pathol. 101, 425–484.
Yajima, T., Knowlton, K.U., 2009. Viral myocarditis: from the perspective of the virus. Circulation 119, 2615–2624.
Yamazaki, T., Akiba, H., Iwai, H., Matsuda, H., Aoki, M., Tanno, Y., Shin, T., Tsuchiya, H., Pardoll, D.M., Okumura, K., Azuma, M., Yagita, H., 2002. Expression of programmed death 1 ligands by murine T cells and APC. J. Immunol. 169, 5538–5545.